Princeton Plasma Physics Laboratory

PPPL-5305

# Energetic particle-driven compression Alfvén eigenmodes and prospects for ion cyclotron emission studies in fusion plasmas

N. Gorelenkov

August 2016

Prepared for the U.S. Department of Energy under Contract DE-AC02-09CH11466.

# Princeton Plasma Physics Laboratory
# Report Disclaimers

---

## Full Legal Disclaimer



## Trademark Disclaimer



---

# PPPL Report Availability

## Princeton Plasma Physics Laboratory:

http://www.pppl.gov/techreports.cfm

## Office of Scientific and Technical Information (OSTI):

http://www.osti.gov/scitech/

---

**Related Links:**

**U.S. Department of Energy**

**U.S. Department of Energy Office of Science**

**U.S. Department of Energy Office of Fusion Energy Sciences**

# Energetic particle-driven compressional Alfvén eigenmodes and prospects for ion cyclotron emission studies in fusion plasmas*

N. N. Gorelenkov

*Princeton Plasma Physics Laboratory,*

*P.O. Box 451, Princeton, NJ, USA 08543-0451*†

## Abstract

As a fundamental plasma oscillation the compressional Alfvén waves (CAW) are interesting for plasma scientists both academically and in applications for fusion plasmas. They are believed to be responsible for the ion cyclotron emission (ICE) observed in many tokamaks. The theory of CAW and ICE was significantly advanced at the end of $20^{th}$ century in particular motivated by first DT experiments on TFTR and subsequent JET DT experimental studies. More recently, ICE theory was advanced by ST (or spherical torus) experiments with the detailed theoretical and experimental studies of the properties of each instability signal. There the instability responsible for ICE signals previously indistinguishable in high aspect ratio tokamaks became the subjects of experimental studies. We discuss further the prospects of ICE theory and its applications for future burning plasma (BP) experiments such as the ITER tokamak-reactor prototype being build in France where neutrons and gamma rays escaping the plasma create extremely challenging conditions for fusion alpha particle diagnostics.

* This manuscript has been authored by Princeton University under Contract Number DE-AC02-09CH11466 with the U.S. Department of Energy. The United States Government retains and the publisher, by accepting the article for publication, acknowledges that the United States Government retains a non-exclusive, paid-up, irrevocable, world-wide license to publish or reproduce the published form of this manuscript, or allow others to do so, for United States Government purposes.

† ngorelen@pppl.gov

## I. INTRODUCTION

Among the papers which initiated fast ion (or energetic particle, EP) physics research and published about fifty years ago several dealt with the cyclotron instabilities [1, 2]. In those and some later studies the fusion ion products drove instabilities dubbed as thermonuclear instabilities.

The cyclotron thermonuclear instabilities are quite unique due their high frequencies and the possibility to tap the energy from fast ions. The excitation of the cyclotron instabilities were treated in a perturbative manner because of relatively small density of energetic particles in fusion plasmas in general,

$$n_h/n_e \ll 1, \tag{1}$$

where $n_h$ and $n_e$ are the densities of fast or hot (subscript "h") ions and the background plasma electrons. In earlier publications it was found that the cyclotron instability could have nonperturbative growth rates, i.e. nonlinear in $n_h$, $\sim \sqrt{n_h/n_e}$ [3, 4]. This stimulated a lot of interest due to potentially strong growth and dangerous effects on the plasma when even small density EP population may have deleterious consequences for the plasma discharge as we discuss below.

An interest in EP cyclotron instabilities emerged after observations of the Ion Cyclotron Emission (or ICE) in tokamaks (see review [5] for experimental and initial theoretical references). ICE is measured by the magnetic field pick up coils at the integer harmonics of thermal ion cyclotron frequency at the low field side of the tokamak. ICE was commonly acknowledged as driven by the super-thermal fast ions such as beam ions, ICRH minority ions, or fusion charged products. In fact some names were introduced associated with the driving species: beam-driven ICE, minority ICRH driven ICE or mICE and fusion product driven ICE (FP-ICE).

Perhaps the most convincing argument in support of ICE excitation by fast ions was presented by Cottrell et al. [6] where it was demonstrated that the intensity of ICE is linearly proportional to the fusion product density for Ohmic and beam-heated discharges over six orders of magnitudes of ICE (and fast ion) power. Similar correlation was reported by JT-60U, TFTR and LHD groups. In some recent LHD experiments, NBI was applied perpendicularly to the direction of the equilibrium magnetic field. In LHD ICE was timed

with TAE excitations [7]. It is Cottrell's publication [6] that brought the attention of the community to the problem of ICE excitation whereas the main elements of ICE theory were already available to a great extent by that time (see review [8]).

Despite the convincing arguments presented by Cottrell[6] in some later studies for example in TFTR the correlation between ICE and neutron signal did not have such linear proportionality. On the contrary, ICE in DT TFTR experiments had more complicated dependences on fusion product density which was not completely understood as pointed out in Ref.[9], although studied theoretically [10, 11]. We should also say that the fast ion cyclotron harmonics do not always coincide with thermal ion harmonics. Examples are $T$ or $He^3$ fusion products in $DD$ plasma or the case of $\alpha$ particle products in $DT$ plasmas.

Similar to the case of cyclotron instability study the development of the ICE theory started from the analysis of the experimentally observed instabilities in the homogeneous limit ignoring the mode structure. In this limit it was assumed that the oscillations have compressional Alfvén (CA) polarization with the dominant parallel component of the magnetic field perturbation. This implied that the plasma displacement is mostly due to the plasma compressibility although coupled to the shear Alfvén branch in toroidal plasma configurations. The interactions between oscillations and the fast ions included realistic drift ion motion [12]. The homogeneous ICE theory was recently reviewed in Refs.[13, 14]. Nevertheless, the limit of the homogeneous plasma allowed to make the case for ICE applications to tokamaks as a diagnostic originally proposed in Refs.[6, 15] (see also recent review [16]).

Later the theory of ICE related instabilities was generalized to include realistic structures of the underlying eigenmodes called later CA eigenmodes or CAEs. We start the review of CAE theory with the relatively recent development of detailed CAE studies in spherical torus (or ST) devices which confirmed the analytic predictions for the eigenmodes dispersion and structure in many respects. This development occurred in early 2000s in connection with ST fusion experiments where ion sub-cyclotron frequency instabilities of CA polarization cavity modes were observed. In particular in NSTX and MAST they were identified as high frequency compressional Alfvénic (or fast magnetosonic) modes driven by fast ions injected by the heating beams [17–22].

In connection with the homogeneous approach to the ICE problem we should say that there are several points worth mentioning which are due to the plasma inhomogeneity. The main point is that CAEs are ubiquitously coupled to kinetic Alfvén waves in realistic plasmas,

see sec. III. This adds to the damping of CAEs and shapes the unstable modes spectrum. Another feature of the inhomogeneous plasma contribution to CAE instability is through the thermal ion cyclotron damping which is straightforward to avoid at certain frequencies which seem to be wider in the case of inhomogeneous plasma. Inhomogeneity also affects the CAE instability due to the fact that spatial variations in the magnetic field broaden the region of the plasma in which thermal ion cyclotron damping can occur.

This review is written in the introductory style. We are giving preference to understanding the physics rather than rigorous derivations of the underlying equations and refer the reader to the original publication references. Mostly we cover the linear physics of ICE instabilities, for which the basics are welldeveloped. The paper is organized as follows. We review first the CAE theory and experiments in ST devices in Sec.II where high, sub-cyclotron frequency modes were analyzed and used to confirm CAE nature of these mode. Then we consider the newly discovered CAE to KAW coupling heuristically in Sec.III as well as its potential applications to ICE problem and thermal electron power channeling. The current status of ICE linear instability theory is summarized in section IV where the plasma inhomogeneity is taken into considerations. Nonlinear progress in ICE theory is briefly discussed in Sec.V. We summarize and discuss the present tasks for ICE theory development in section VI.

## II. OBSERVATIONS OF HIGH FREQUENCY MODES IN STS SUPPORT ICE INTERPRETATIONS

Initial studies of cyclotron instabilities responsible for the Ion Cyclotron Emission (ICE) were based primarily on the analysis of the high frequency spectra of the Mirnov magnetic signal. The studies showed that the underlying fluctuations are of Alfvénic nature, driven by super-Alfvénic ions and the resonances are cyclotron with the Doppler shift. These properties helped to identify the magnetic activities as the cyclotron instabilities of the Compressional Alfvén Eigenmodes (CAEs, also called fast Alfvén or magnetosonic eigenmodes) [23–27].

We should note that another kind of plasma oscillations could be, in principle, a candidate to explain the ICE observations, namely the shear Alfvén eigenmodes. However they are known to be heavily damped due to strong interaction with the Alfvén continuum. Only at frequencies, much lower than the thermal ion cyclotron frequency, can the shear Alfvén modes can be formed without strong continuum damping [28, 29].

In STs the shear Alfvén eigenmode instabilities with the frequencies comparable to the cyclotron frequency of thermal ions correspond to the excitations of the so-called global shear Alfvén (GAE) [30] modes. It is now believed that the instabilities of GAEs have sub-cyclotron excitations, i.e. $\omega_A = \omega_{cA} k_\parallel / k_\perp < \omega_{ch}$, whereas CAEs might be excited at higher frequencies (at and above $\omega_{ci}$) [31]. CAEs are used to explain the ICE phenomena in tokamaks [25–27]. Here we denoted the shear Alfvén frequency as $\omega_A$, the frequency of the compressional Alfvén wave branch as $\omega_{cA}$ and the hot ion and thermal ion cyclotron frequencies as $\omega_{ch}$ and $\omega_{ci}$ (also denoted as $\omega_c$ if the distinction is not required).

Significant progress in studies of CAE properties was made in ST tokamaks by exciting the sub-cyclotron instabilities in a beam heated discharges. Observations of CAEs in STs allowed the measurements of the dispersion and the polarization properties of a single ICE relevant instability including their internal structures. The main reason for this is the intrinsically low equilibrium magnetic field in STs, so that the frequency spacing between the neighboring CAEs, $\delta f \sim v_A / r$, is small but measurable [17]. Because of the importance of CAE dispersion and structure we will introduce them next. First we will cover this topic's theory in the next section according to its present understanding.

### A. Heuristic introduction to CAE theory

Let us illustrate the basics of the CAE theory heuristically following earlier publications [24, 25] (see also Ref. [20]). In particular, in Ref. [24] the eigenmode equation was postulated (later derived more rigorously in Ref.[25]) taking the right-hand side (RHS) of the following compressional Alfvén wave dispersion

$$\omega_0 = n\omega_c = \omega_{cA} \equiv k_\perp v_A, \tag{2}$$

to the second power and making use of the standard inequality for tokamaks, $k_\parallel / k_\perp \ll 1$. Within the approximation of this section we can readily treat the CA dispersion as an operator acting on the dominant magnetic perturbation $\hat{k}_\perp^2 \delta B_\parallel = (\omega_{cA}^2 / v_A^2)\, \delta B_\parallel$ since for CAEs the dominant perturbed quantity is the parallel component of the equilibrium magnetic field, $\delta B_\parallel$:

$$\frac{1}{r}\frac{\partial}{\partial r} r \frac{\partial}{\partial r} \delta B_\parallel + \frac{1}{r^2}\frac{\partial^2}{\partial \theta^2} \delta B_\parallel = -\frac{\omega^2}{v_A^2(0)} \frac{n(r)}{n_0} (1 + \epsilon \cos\theta)^2 \delta B_\parallel, \tag{3}$$

where $r$ is the radial coordinate, $\theta$ is the poloidal angle, $\epsilon = r/R$ is the inversed aspect ratio of the plasma column, and the plasma density profile is introduced via $n(r)$. Pure CAE polarization limits the analysis by ignoring the interaction with the shear Alfvén branch which we consider in the next section.

The RHS of this equation has the minimum at the localization region of the mode structure as illustrated in Fig.(1). Typically this is at the edge of the plasma being elongated vertically in the poloidal direction. Radially localized normal mode solutions of Eq.(3) can be found by considering that the potential well is formed with the narrow radial width and shallow but long poloidal extension. In other words CAE poloidal wavelength is shorter than the radial wavelength. This justifies the choice of the eikonal for the following poloidal mode structure (cf. [24]):

$$\delta B_{\parallel}(r,\theta) = b(r,\theta)\exp\left[-i\omega t + im\left(\theta + \epsilon_0 \sin\theta\right) - in\varphi\right], \tag{4}$$

where $\varphi$ is the toroidal angle, $m$ is the poloidal mode number, and the subscript 0 denotes the value taken at the minimum of the local effective potential well, $r = r_0$ (~~the definition is~~defined after Eq.(6)). We should note here that because of the potential well poloidal elongation CAEs (see illustration of this in STs in Ref.[20]) have the following ordering for its wave-vectors

$$k_\theta \gg k_\varphi \gg k_r, \tag{5}$$

which is supported by the CAE stability theory.

The poloidal mode number is assumed to be large so that the equation for CAE mode amplitude, $b(r,\theta)$, implies slow variation in both directions but sill requiring $\partial b/\partial \ln r \gg \partial b/\partial\theta$. The envelop of CAE mode structure can be found iteratively with zeroth iteration accounting only for the poloidal variation in the eikonal (4). Introducing the plasma density dependence as $n(r) = n_0\left(1 - r^2/a^2\right)^{\sigma_i}$, the first and second iterations produce the solution envelops [32]

$$b(r,\theta) = b_0\phi_k\left(\frac{\sqrt{2}\theta^2}{\Theta}\right)\phi_s\left(\frac{\sqrt{2}\,(r-r_0)}{\Delta}\right), \tag{6}$$

where $\phi_s$ is the Chebyshev-Hermite function and the characteristic widths of those functions are $\Theta^2 = 1/\left(\epsilon_0 - \alpha_0\right)(m+1/2)$, $r_0^2/a^2 \simeq 1/(1+\sigma_i)$, and $\Delta^2/a^2 = \kappa\sqrt{2\sigma_i/(1+\sigma_i)\left(\epsilon_0-\alpha_0\right)}/(2m+1)$, where $\alpha_0 = B_\theta^2/2B_\varphi^2$. The assumptions of Ref.[32] included $m \gg nq(r_0)$ and $\varepsilon > 1-\kappa^2$.

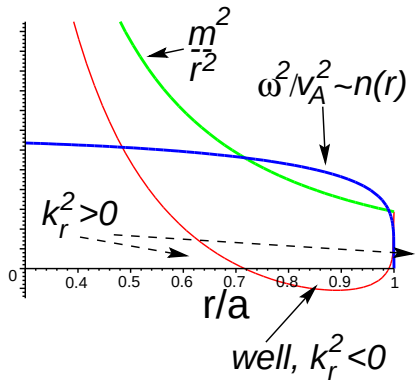


Figure 1. *CAE potential well radial dependence (in a.u.)* ~~*is indicated on a graph*~~ *and is given by the* ~~*sum of*~~ *the RHS of Eq.*(3) *(blue curve) and the poloidal wave-vector* $m^2/r^2$ *(green curve). The potential well is formed by the plasma density profile and the poloidal eikonal* $m^2/r^2 - \omega^2/v_A^2$*. The radial wavelength is defined via the operator* $k_r^2 = -r^{-1}\,(\partial/\partial r)\,r\,(\partial/\partial r)$*.*

A variational method of solving the eigenmode equation (3) was adopted in Ref. [33]. It assumes low $m$ values. While for $\Delta/a$ Ref. [33] has found a similar to Eq.(6) expression for the poloidal localization the expression was somewhat different, namely:

$$\Theta^{-4} \simeq n^2 q^2 \left(\kappa^2 - \frac{R_0}{R}\right),$$

where we show only the leading order terms in $n^2$.

Although the poloidal mode number dependence is the same in both treatments the numerical factors are different, in part due to the expected eikonal of Ref. [32] being enforced by Eq.(4). Predictions for the mode frequency as a function of CAE mode numbers are also different. The dominant reason for this is that the used poloidal number $m$ in Ref.[32] was consistent with employed approximation.

Because of the complexity of the above eikonal the realistic CAE dispersion as we will see is difficult to analyze and compare with experiments. For example, in the aforementioned papers [32, 33] used theoretical methods are rather approximate since they are based on the assumption of the eikonal. Instead a heuristic dispersion relation of CAEs adopted in Ref. [34], by analogy with the dispersion (2), finds the characteristic length and corresponding "quantum" numbers in each three relevant directions: toroidal mode number, $n$, with the major radius $R$ being the characteristic length; radial mode number, $S$, with the radial width of the effective potential in radial direction, and$m$, with the plasma minor radius giving the characteristic length. One can write then

$$\omega^2_{MSn} \simeq v^2_A \left( \frac{m^2}{r^2} + \frac{S^2}{L^2_r} + \frac{n^2}{R^2} \right). \tag{7}$$

The numerical solutions obtained in Ref.[34] using the ideal MHD code NOVA agreed with the dispersion relation (7) which in its turn is consistent with the eikonal (4). The above dispersion was checked numerically only for $n = 0, 1$ due to strong coupling of the dominant compressional Alfvénic polarization of CAEs and the shear Alfvénic harmonics at higher $n$ numbers.

Another paper, Ref.[35], within the used model debated the validity of the above approach which is based on the eikonal Eq.(4), although the treatment of Ref.[35] does not seem suitable for large ellipticity tight aspect ratio plasmas. More recently CAE studies were dealt with the ST plasmas where the authors managed to decouple the shear Alfvén and the compressional Alfvén plasma oscillations [36]. The obtained equations are for "pure" CAEs, i.e. ignoring the interactions with the kinetic Alfvén waves (KAW) and thus ignoring the important dissipation mechanism for CAEs with the sub-cyclotron eigenfrequencies. The interaction was recently considered as a way to channel the energy from beam ions to thermal electrons [37]. This mechanism is covered in the next section.

Nevertheless, the modeling of pure CAEs was very important for the interpretation of the experimental results from NSTX and MAST experiments. CAE dispersion of Eq.(7) was brought into consideration in Refs. [17, 21, 34]. The comparison with the experiments illustrated clear frequency separation for the modes at subsequent "quantum" numbers of CAEs according to Eq.(7). These CAE dispersion properties were validated after ST experimental measurements of high frequency sub-cyclotron instabilities were interpreted [17, 32]. Moreover, the CAE dispersion seems to be instrumental in helping experimentalists identify the kind of the instabilities by following the mode frequency evolution, i.e. their dispersions, without unambiguously knowing the polarizations [38].

We show examples of CAE observed magnetic field signals from NSTX and MAST devices in left and right Figs. (2) respectively. In the left figure from NSTX, two CAE unstable peaks cluster clearly around $1MHz$ and $2MHz$, which corresponds to the largest frequency separation, $\sim 1MHz$, associated with the radial mode number $S$ (see Eq.(7)). Smaller frequency separation is due to the poloidal mode number, $\Delta f \simeq 120kHz$, whereas the smallest separation in frequency could also be distinguished around each peak in the left figure (2). It is due to the toroidal mode number $n$ at $\Delta f \simeq 20kHz$. Similar frequency

separations were reported in Ref.[33] which is mentioned above.

An experimental study of CAE modes on MAST was done in a similar manner and is illustrated in the spectrogram of the right figure (2). Although the spectrogram shows the low part of the frequency spectrum, clear peaks indicated by their toroidal mode numbers correspond to the ICE unstable CAEs at much higher frequencies. The values of those CAE frequencies were recovered by assuming that measured signals are actually aliases of real peaks. The inferred values of the frequency separation were similar to the values seen in NSTX. That is, the poloidal mode number separation is on the order of $150kHz$ and, the toroidal mode numbers are separated by $\Delta f = 10 - 15kHz$, whereas the whole observed band is estimated at the value of its frequency $f = 1 - 2MHz$.

At first glance the spectra shown in Figs.2 resemble the harmonics of ICE: discrete peaks in the Mirnov coil spectrum, almost equally spaced in frequencies. However the edge cyclotron frequency of the background thermal deuterium ion was $\sim 2.2MHz$ in NSTX and $\sim 2.5MHz$ in MAST in those shots which are much larger than the peak frequency separation shown in the figures. Nevertheless the frequency separations corresponding to various mode numbers as we highlighted served as an important confirmation of CAE's dispersion and their theory. It potentially allows the development of diagnostics to study fusion plasmas and burning plasmas in particular as we will be discussing below (discussion on ICE as a diagnostic for fusion is presented in Sec.VI).

Due to this understanding the CAE theory helped to offer the ways for its validations in spherical tokamaks. Furthermore, Ref. [36] offered the method of how to decouple the CAE eigenmode problem from problem of shear Alfvén waves. This allowed to focus on the "pure" CAE properties only. A similar approach with slightly further reduced model was developed and applied to the MAST plasma [39]. In that work co- and counter- propagating solutions in the direction of the plasma current are reported. Let us illustrate those studies by showing the numerically computed CAE mode structures in Fig. (3). The shown CAE modes have the mode structure similar to the one we used in this review (see Eq.(6)). Both theoretically [40] and numerically [36] CAEs that were localized at the high field side (HFS) were also reported.

Above we demonstrated radial localizaton of CAEs (see illustration on Fig.1). Poloidal CAE localization can be seen from the poloidal variation of the effective potential well (see

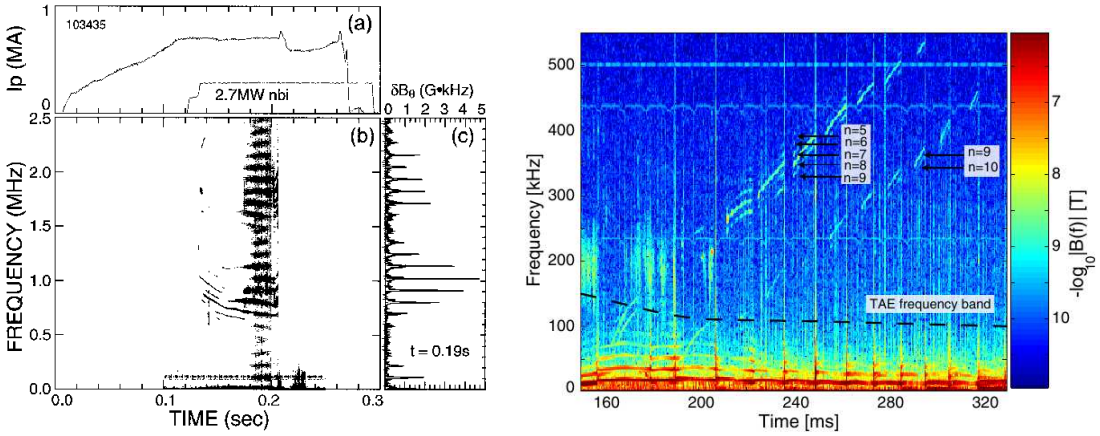


Figure 2. *Two representative spectra of CAE activity seen on NSTX [17] (left), and MAST [21] (right) are shown. The spectra were measured by the pick-up magnetic field (or Mirnov) coils installed just outside the plasma. The MAST spectrum depicts the toroidal mode numbers corresponding to the smallest frequency splits between the signals as indicated.*

Eq.3), i.e. the solution is bounded in poloidal direction by zeros of the potential well [20]:

$$\frac{m^2}{r^2} - \frac{\omega^2}{v_A^2(0)} \frac{n(r_0)}{n_0} \left(1 + \frac{r_0}{R}\cos\theta\right)^2 = 0.$$

The critical role of the aspect ratio on the poloidal localization of CAEs was studied in Ref.[36]. In particular in a high aspect ratio plasma, i.e. in a so-called "tokamak" approximation, the poloidal localization could not be seen. However in ST-like devices, at $R/a \sim 1.3$, CAEs were found to be well localized on the low field side. This is similar to the results reported by the WHALES code which are also shown in Fig.3.

Finally we summarize this section by stating that it is due to CAE observations in ST devices and to theoretical advances that it became possible to understand the nature of modes responsible for ICE.

## III. CAE TO KAW COUPLING

We proceed here in the spirit of the heuristic analysis introduced in the previous section in the case of sub-cyclotron CAE frequency. But first let us show the example of CAE/KAW coupling for the sub-cyclotron frequency case which was found recently in Ref.[37]. The results are from the initial value hybrid MHD/kinetic fast ions code HYM simulations of CAE/KAW structure in NSTX plasma as shown in Fig.4. The left figure clearly depicts

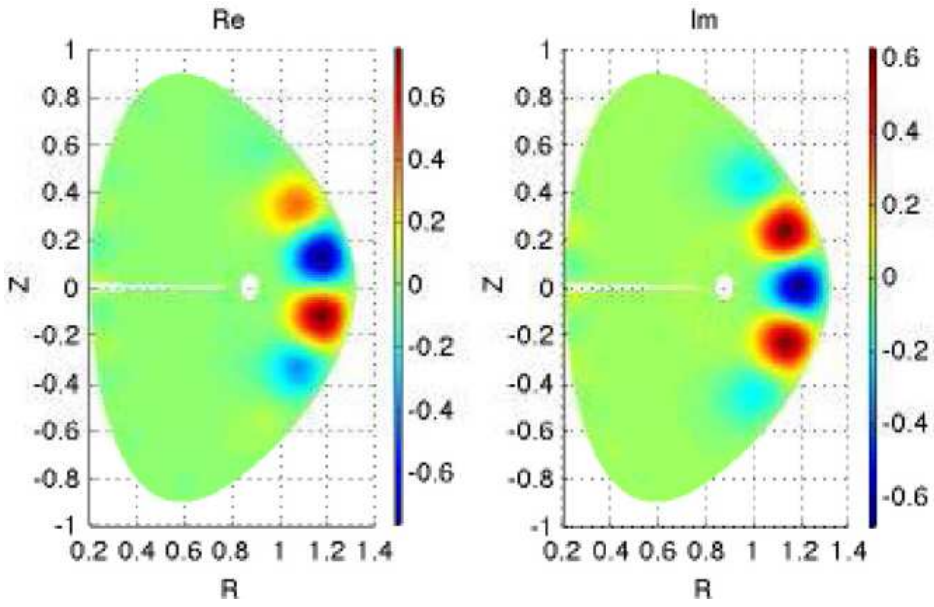


Figure 3. *Poloidal structure of the CAE mode computed by the code WHALES. We are showing the real and imaginary values as indicated on the graph of the variable* $\eta_*$*. It represents the normal to the magnetic surface component of the plasma displacement. The depicted mode corresponds to* $n = 10$ *and the mode frequency* $f = 2.23MHz$*.* [39].

the dominant CAE structure which is mostly $\delta B_{\parallel}/B$ perturbation whereas KAW is represented primarily by the $\delta B_{\perp}/B$ perturbation. Shown CAE structure is similar to pure "CAE polarization" mode from the previous section computed by the WHALES code. More complete analyses using HYM code has discovered an additional excitation of the kinetic shear Alfvén wave structure at a point of CAE and KAW local frequency resonance. It can be seen that the resonance occurs at the HFS in the mid-plane and the KAW structure propagates poloidally until it damps. The wave-vector of KAW as expected has dominant $\boldsymbol{k}_{\theta}$ which is clearly follows from figure 4 where part of the eigenmode KAW structure propagates poloidally. Another important point to make here is that KAW structure is relatively narrow which means that all the energy is in the CAE component of the solution.

For further analyses, the CAE eigenvalue problem represented by equation (3), needs to be corrected to account for more complete system which allows the coupling to KAWs. We include small radial scale contributions, i.e. fourth order radial derivatives following Refs.[41, 42]. The exact form of that is not important as we argue below. What is important is how much power from CAE is available to channel to KAW structure since all the power

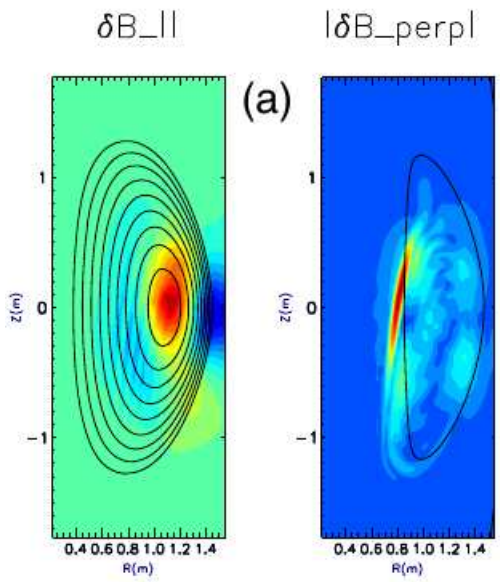


Figure 4. *n=8 CAE coupled to KAW in NSTX plasma as computed by the HYM code. Shown on the left is the parallel component of the perturbed magnetic field representing the CAE structure. Right figure depicts $\delta B_\perp$ corresponding to the KAW part of the mode. Black curves correspond to the magnetic surfaces on the left and the CAE/KAW resonant surface on the right, i.e. Eq.*(9)*. The mode frequency is $\omega = 0.48\omega_{ci}$.*

is absorbed[37].

Let us do several transformations to Eq.(3). First, we rewrite it in terms of the perturbed electric potential $\phi$ [25]. Then we multiply it by by $\omega^2 - k_\parallel^2 v_A^2$ which will account for local shear Alfvén resonances [43]. And we add the fourth order derivative in radius following Refs.[41, 42]. Finally we obtain a CAE/KAW eigenmode equation to understand the HYM obtained hybrid solution

$$\begin{gathered} k_\parallel^2 v_A^2 \rho^2 \frac{\partial^4}{\partial r^4}\phi + \frac{\partial}{\partial r} r \left(\omega^2 - k_\parallel^2 v_A^2\right) \frac{\partial}{\partial r}\frac{\phi}{r} = \\ = \left(\omega^2 - k_\parallel^2 v_A^2\right) \left[-\frac{1}{r^2}\frac{\partial^2}{\partial \theta^2} - k_\parallel^2 - \frac{\omega^2}{v_A^2(0)}\frac{n(r)}{n_0}\left(1+\epsilon\cos\theta\right)^2\right]\phi \end{gathered}, \tag{8}$$

where $\rho^2 = \left[3\omega^2/4k_\parallel^2 v_A^2 + (1-i\delta)\,T_e/T_i\right]\rho_i^2$ and $\rho_i$ is the thermal ion Larmor radius.

Let us note here several important points. First is that KAW is not an eigenmode but a propagating part of the eigenmode structure. Second note is that the CAE/KAW equation is important to analyze in order to understand its consistency with some limiting cases. One such case is the MHD and $k_\parallel^2 v_A^2 \ll \omega^2$ condition limits when one can drop the first term and straightforwardly arrive at the CAE eigenmode equation, Eq.(3). However if we keep

$k_\parallel$ at finite value and assume that $\omega^2 \sim k_\parallel^2 v_A^2$ we arrive at the shear Alfvén equation such as discussed in Ref.[44]. For our analysis Eq.(8) is sufficient because it illustrates the coupling of two fundamental MHD branches. We will also add here that the equation similar to Eq.(8) was obtained and analyzed in Ref. [43] in the limit of one-dimensional plasma of the magnetosphere.

We also note that the KAW local dispersion is covered in Swanson's textbook [45] as well as in a more recent preprint [46] where KAW dispersion was accurately evaluated at frequencies well above $\omega_c$, i.e. when thermal ions are unmagnetized. Thus, the CAE to KAW power channeling problem is relevant for ICE at arbitrary frequencies but needs to be specially addressed which is beyond the scope of this review. The frequency of propagating KAW structure of CAE eigenmode satisfies the following dispersion relation found within the HYM code simulation model:

$$\omega^2 = k_\parallel^2 v_A^2 \left[1 + \frac{n_h}{n_e}\left(\frac{3k_\perp^2\rho_h^2}{4} - \frac{\omega^2}{\omega_c^2}\right)\right], \tag{9}$$

as assumed in Ref.[37] where the model includes FLR contributions from beam ions only. But more sophisticated modeling should expand used assumptions and include thermal ion FLR as well as thermal electron contributions which generalize KAW dispersion to

$$\omega^2 = k_\parallel^2 v_A^2 \left[1 + \frac{n_h}{n_e}\frac{3k_\perp^2\rho_h^2}{4} + \frac{3k_\perp^2\rho_i^2}{4} + k_\perp^2\rho_s^2 - \frac{\omega^2}{\omega_c^2}\right], \tag{10}$$

where $\rho_s$ is the sound gyro-radius.

Eq.(8) can be solved using the asymptotic analysis [41] where the radial domain is sub-divided with two scales characterizing the solution: the MHD scale corresponding to the balance of the second and the last terms of Eq.(8),

$$\begin{gathered} \tfrac{1}{r}\tfrac{\partial}{\partial r} r\left(\omega^2 - k_\parallel^2 v_A^2\right)\tfrac{\partial}{\partial r}\phi = \\ = \left(\omega^2 - k_\parallel^2 v_A^2\right)\left[-\tfrac{1}{r^2}\tfrac{\partial^2}{\partial\theta^2} - k_\parallel^2 - \tfrac{\omega^2}{v_A^2(0)}\tfrac{n(r)}{n_0}\left(1+\epsilon\cos\theta\right)^2\right]\phi \end{gathered}, \tag{11}$$

and near the resonance point $r_{res}$ of the frequencies match, $\omega_{cA}^2 = k_\parallel^2(r_{res})\, v_A^2$, the kinetic scale corresponding to the first and second terms balance,

$$k_\parallel^2 v_A^2 \rho^2 \frac{\partial^2}{\partial r^2}\phi' + \left(\omega^2 - k_\parallel^2 v_A^2\right)\phi' \simeq 0, \tag{12}$$

where $\phi' \equiv \partial\phi/\partial r$. The CAE part of the eigenmode away from $r_{res}$ is found by solving Eq.(3) which has the 2D mode structure (4) and (6). Then near the resonance location we

expand $\omega^2 - k_\parallel^2 v_A^2 \equiv \omega_{cA}^2 x\,(\delta/L_r)$, where $x = (r - r_{res})/\delta$, $L_r$ is given by the radial profile of the plasma density and the safety factor, and $\delta^3 \equiv \rho^2 L_r$.

In new variables Eq.(12) has the following form

$$\frac{\partial^2}{\partial x^2} E_r + x E_r + (L_r/\rho)^{2/3} (k_\theta/k_r) E_\theta = 0, \tag{13}$$

where $E_{\theta,r}$ are the poloidal and radial components of the perturbed electric field and are determined by the CAE mode structure near the CAE/KAW resonance point. This equation is similar to the one analyzed in Ref.[47]. The role of the external field plays the poloidal component of the CAE part of the solution, $E_\theta$. Together with the radial part of CAE electric field, $E_{rcA}$, it can be expressed via the dominant magnetic perturbed component [48]

$$E_{rcA} \simeq \frac{\omega}{c k_\theta} \delta B_\parallel = \frac{k_r}{k_\theta} E_\theta \simeq i k_r \phi. \tag{14}$$

The KAW part is found following Ref.[47] (coefficients of this equation differ from [47], their derivation will be published elsewhere),

$$E_r = -\frac{E_\theta k_\theta}{k_r} \left(\frac{L_r}{\rho}\right)^{2/3} \sqrt{\pi} \left(\frac{\delta}{r}\right)^{1/4} \exp\left\{ i \frac{2}{3} \left(\frac{r}{\delta}\right)^{3/2} + \frac{\pi}{4} \right\} + \frac{E_\theta k_\theta}{k_r} \frac{L_r}{r}, \tag{15}$$

for $r > r_{res}$ and

$$E_r = \frac{E_\theta k_\theta}{k_r} \frac{L_r}{r}, \tag{16}$$

for $r < r_{res}$.

Finally we summarize the above analysis for the solution of the CAE/KAW eigenmode problem. It is given by the combination of CAE dominated structure, Eqs.(4,6), together with KAW propagating solution, Eqs.(15,16). It can be seen that the found solution is consistent with the solution found by HYM (see Fig.4). Its KAW structure is propagating mostly poloidally due to $k_\theta \gg k_r$ and is quickly absorbed by the surrounding thermal plasma. Its mathematical formulation can be improved using the Umov-Poynting vector formalism [49, 50]. Not everything is understood in HYM numerical CAE/KAW solutions, in particular the poloidal KAW localization as well as the magnitude of its damping rate on thermal electrons.

Depending on the needs of the analysis the above CAE/KAW solution can provide either damping rate or power channeling to thermal electrons. The damping implications for CAEs is due to relatively short radial wavelength of KAW structures i.e. $k_\perp \rho_i \sim 1$, which have

strong parallel electric fields and strong power channeling to the electrons. We should note that this mechanism was overlooked in the conventional ICE theory. The CAE to KAW power channeling is an important dissipation mechanism which has to beconsidered in codes targeting CAEs.

## IV. ICE AS A CAE INSTABILITY

Among many candidates for ICE discussed earlier[5] the most probable is the CAE cyclotron instability driven by the velocity space anisotropy of super-thermal ions. In section II A the CAE theory was reviewed using the ideal MHD eigenmode equations which are sufficient to interpret and understand the experimental data from tokamaks and STs. It was shown more recently that for more accurate treatment of the modes the Hall term has to be included in the CAE framework to compute the dependence of the solutions on the poloidal phase velocity [27, 51, 52]. One particular consequence of this is the shift of the eigenmode frequencies depending on the sign of $m$. For the plasma cross section with the ellipticity $\kappa$ the eigenfrequencies of CAEs were found to be asymmetric with respect to poloidal mode number sign [27]:

$$\omega_{CAE} = k\left(\kappa\right) v_A\left(r_0\right) \left[ \frac{\sigma_m v_A \left(\ln n\right)'}{2\bar{\omega}_c} + \sqrt{1 + \left( \frac{v_A n'}{2\bar{\omega}_c n} \right)^2} \right]_{r_0}, \tag{17}$$

where the location of the eigenmode is given by the equation

$$2 + r\left(\ln n\right)' - \sigma_m \frac{v_A}{\bar{\omega}_c} \left( r\left(\ln n\right)' \right)' \sqrt{1 - \frac{2 + r\left(\ln n\right)'}{\left( r\left(\ln n\right)' \right)'}} = 0, \tag{18}$$

and as above $\left(\ldots\right)' \equiv \partial\left(\ldots\right)/\partial r$. Other notations here are: $k\left(\kappa\right) = \left|m\right| \sqrt{\frac{1+\kappa^{-2}}{2}}/r$ is the poloidal wave vector, $\bar{\omega}_c \equiv \omega_c \sqrt{\frac{1+\kappa^2}{2}}$ is the cyclotron frequency, and $\sigma_m = m/\left|m\right|$ is the sign of the poloidal wave number. Further analytic and numerical treatments of CAE eigenvalue problem can be found in Ref.[40]. As we point out in the discussion section VI the dispersion 17 should be important in ICE applications for possible diagnostics of burning plasmas since this will affect the stability of the CAE modes and will certainly modify ICE spectrum.

A theory of CAE instabilities driven by super-Alfvenic ions in applications to ICE is developed for various cases. Below we highlight its main elements following the author's earlier works [25, 48]. They were strongly influenced by A.B. Mikhailovskii reviews on

cyclotron instabilities by fast ions and in particular by Ref. [8]. A similar approach to CAE instabilities was developed in Ref. [53], where the slow instability limit was implied although no applications to ICE in experiments were made. Other papers dealing with ICE instabilities were limited to the strong instability as discussed below [10, 26] (see also recent publications on those interactions in strong instability limit Refs.[13, 14] and in earlier papers [12, 15]). More recent formulations of CAE growth rates in applications to STs analyze the growth rate expressions accounting for EP drift frequency contributions which carefully address not only the cyclotron but EP drift frequencies [54, 55].

Nevertheless the CAE growth rates and their derivations are common for cited publications. However one difference exists which is how the instability is considered: being strong or weak. There are two known theoretical limits of ICE theory with respect to the instability growth rate. The first one is the strong CAE instability theory when the mode grows faster than the EP drift motion or the growth rate satisfies $\gamma > \Delta\tau^{-1}$, where $\Delta\tau = min\left(\tau_{res}, \Theta qR/v_{\|}\right)$ is the characteristic time of wave-particle interaction, $\tau_{res}$ is the time of particle interaction with the perturbation near the local resonance, $\Theta qR/v_{\|}$ is the time which the particle spends in the localization domain of the unstable mode. Here we followed the line of arguments of Ref. [18] where the example of NSTX plasma was used for which $\Delta\tau = 0.7 \times 10^{-6}s$ is found at $\Theta = 1$, $R = 100cm$, $q = 1$, and $\chi = 0.5$ (pitch angle, $\chi = v_{\|}/v$). The validity condition for the strong instability theory in NSTX example is then:

$$\frac{\gamma_{CAE}}{\omega} > 0.1\frac{\omega_c}{\omega}.$$

The second limit is known as the slow instability limit. In it the EP drift motion should be included in the wave-particle interaction. The cyclotron instability example considered above is of the first type, i.e. it is the strong instability. The instabilities of this type were proposed to explain ICE in TFTR and in JET DT tokamak experiments in Refs. [10, 26]. In fact, in both papers a smooth transition from the linear or perturbative in EP density dependence of the growth rate to square root dependence is found numerically at $n_h/n_e \sim 10^{-6}$. Such and even higher values of EP density were reported for TFTR experiments but no clear picture of ICE signal transition to square root dependence was demonstrated using the experimental data [9]. ICE signal delay shown in Fig.6 of Ref.[6] clearly exhibits a linear dependence of ICE signal vs. $n_h/n_e$ in JET DT plasmas. Experimentally it may not be straightforward to determine in which regime, weak or strong, the CAE instability is excited.

This is because the instability can likely be observed in the saturated nonlinear state which is only beginning to be developed and is beyond the scope of this review. Nevertheless both regimes are important to distinguish theoretically to compute CAE growth rates.

CAE growth rates are typically computed via the anti-Hermitian part of the permeability tensor of species $j$, $\hat{\boldsymbol{\epsilon}}_j^A$:

$$\gamma \simeq -\frac{\omega}{2}\frac{\sum_j \Im \int E_1^* \hat{\epsilon}_{j11}^A E_1 d^3r}{\int E_1^2 \left|\hat{\epsilon}_{11}\right| d^3r}, \tag{19}$$

where $E_1$ is the component of the perturbed electric field in the direction of the mode propagation which is expected to be poloidal if $k_\theta \gg k_r$, and the integration is taken over the plasma volume occupied by the mode. The permeability tensor appears in the above expression for the anti-Hermitian part of the perturbed current, $\tilde{\boldsymbol{j}}^A$, of plasma species $j$ which in its turn can be expressed via the perturbed distribution function:

$$\int E_1^* \hat{\epsilon}_{j11}^A E_1 d^3r = \frac{4i\pi}{\omega}\int \boldsymbol{E}^* \cdot \tilde{\boldsymbol{j}}^A d^3r = \frac{4i\pi}{\omega} e \int \boldsymbol{E}_1^* \cdot \boldsymbol{v}_\perp \tilde{f}_j d^3v d^3r, \tag{20}$$

where $\boldsymbol{v}_\perp$ is the vector of the perpendicular particle velocity, $\tilde{f}_j$ is the perturbed distribution of species $j$. Then after some algebra one arrives at (for more complete derivation we refer to Ref.[48])

$$\int E_1^* \hat{\epsilon}_{11}^A E_1 d^3r = -\frac{8\pi^2 e^2 B}{\omega_c \omega^2 T}\int dP_\varphi d\mu d\mathcal{E}\tau_b \sum_{l,p}\frac{F_{lp}'^* \left(\omega - \omega_*^T\right) F_{lp}}{\omega - l\bar{\omega}_c - \bar{\omega}_D - p\omega_b} f, \tag{21}$$

where we dropped subscript $j$ which refers all the relevant terms to $j$ species. Here we made use of the set of COM (constants of motion) variables, $\mathcal{E}$ - particle energy, $P_\varphi$ - toroidal canonical momentum, $\mu$ - adiabatic moment, and denoted $\tau_b$ the ion drift bounce (or transit - for passing particles) frequency, $f$ the equilibrium distribution function, and the functions $F_{lp}'$ account for the wave particle interactions[48], the set of frequencies in the denominator includes CAE eigenfrequency, cyclotron, drift and drift bounce frequencies. A similar expression was obtained earlier by Mikhailovskii[8] in the limit of zero banana width for well-trapped and strongly passing ions. This equation contains the bounce resonances of slow growing CAE mode. They were summed in the following novel way [48].

The resonant denominator in Eq.(21) is expandable into the integrable form involving the delta function of the resonance condition:

$$\frac{1}{\omega - l\bar{\omega}_c - \bar{\omega}_D - p\omega_b} = \frac{\mathcal{P}}{\omega - l\bar{\omega}_c - \bar{\omega}_D - p\omega_b} - i\pi\delta\left(\omega - l\bar{\omega}_c - \bar{\omega}_D - p\omega_b\right), \tag{22}$$

where $\mathcal{P}$ denotes the principal part of the integral. The delta function makes it possible to ~~to~~ transform and integrate the sum over the bounce harmonic: integer $p$. Finally the expression for the growth rate of the CAE mode becomes

$$\frac{\gamma}{\omega_c} = \frac{\omega^3}{\omega_p^2 \omega_c^2} \frac{\sqrt{2} ecB}{\sqrt{\pi} \Delta r_0 R_0} \sum_{l,\sigma} \int dP_\varphi d\mathcal{E} d\mu I^2 \frac{E_1^2}{E_0^2} \frac{\mu l J_l^2(z)}{z^2} \left[ \frac{\partial}{\partial \mathcal{E}} + \frac{l\omega_c}{\omega B} \frac{\partial}{\partial \mu} \right] \tilde{f}, \tag{23}$$

where $\omega_p$ is the plasma frequency, $E_1 = E_0 f(r,\theta)$ is the CAE structure in the poloidal cross section required for proper averaging of the local growth rate expression, $\Delta$ is its radial width, $J_l$ is the Bessel function of order $l$ of the argument $z = k_1 \rho_h v_\perp / v$, and $\rho_h$ is the Larmor radius of the fast ions. The resonance condition is then $\omega - l\omega_c(r,\theta) - \omega_D(r,\theta) = 0$ which is to be evaluated along the EP drift trajectory. This resonant condition is different from the resonance in (22) by the bounce harmonics term $p\omega_b$ which is summed over with the novel technique by substituting it with the integration over $\mu$. That is in the model assumption the harmonics number is large whereas the cyclotron resonance is implicitly included in Eq.(23). Also a special function involving the time derivative of fast ion local ~~freqeuncies~~frequencies is introduced $I^2 = 8\pi / \left| \frac{d}{dt} (l\omega_c + \omega_D) \right|$ and is to be taken at the point where the ion has the cyclotron resonance with the mode (for more details see [48]). The term $I$ has the dimension of a time and determines how long the particle was in a resonant layer.

An important element of ICE theory is the quest for the dampings which can shape the spectrum of unstable CAEs in linear simulations. Several damping mechanisms were considered in recent publications on the alpha channeling [56], including thermal electron and ion Landau cyclotron resonant dampings. However, as we said above in Sec.(III), an important and often dominant damping mechanism is the coupling of the KAW structures to CAEs [37], which was previously overlooked in ICE studies. As we show in Sec.10 KAWs induce damping of CAE modes which can be very large, on the order of the mode frequency. Another damping mechanism which depends on thermal ion FLR is the cyclotron damping due to the interaction with the Bernstein waves [12]. It can be minimized in tokamaks since thermal ions have small velocities and thus small Doppler shift. However the power channeling to KAW is argued to be ubiquitous in toroidal geometry[37]. As a result CAE instability linear theory needs to be revisited in view of this finding.

In connection with CAE dampings we would like to note that CAE instabilities do not necessarily lead to ICE. They can occur at arbitrary frequencies between the integer har-

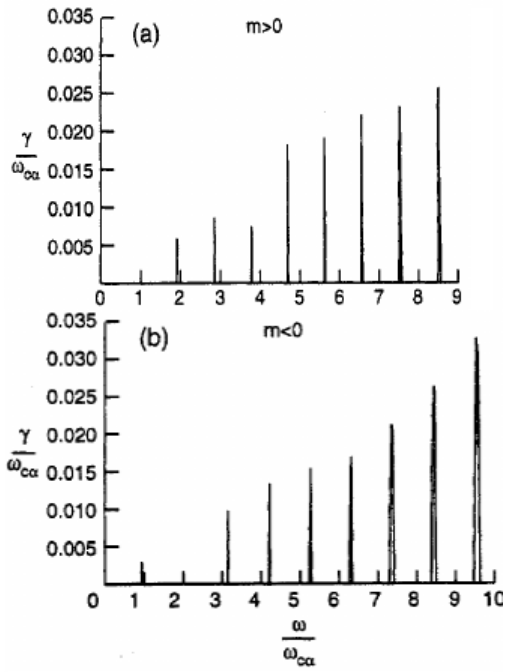


Figure 5. *ICE spectrum computed for JET parameters excited by fusion products, $\alpha$-particles. Two classes of CAE instabilities are shown with the negative (figure (a)) and positive (figure (b)) poloidal mode numbers as noted in the figures. Showing both figures we made the horizontal axis to be on the same scale.*

monics of plasma ion cyclotron frequency, $\omega \neq l\omega_c$. However it is believed that the further away from the exact cyclotron resonance the CAE frequency is the less important thermal ion damping becomes which helps to shape the ICE spectrum. A substantial discussion on allowed CAE eigenfrequencies from the point of view of the mode damping on thermal ions and electrons is presented in Ref.[56].

Let us illustrate the linear ICE growth rate calculations performed in Ref.[26] by showing CAE instability leading to ICE in Fig. (5). One can note a doublet lines near each of the cyclotron harmonic. This feature of ICE exists in experiments and was considered in Ref.[26] in particular. One can also note that closer to low number harmonics of $\omega_c$ the instability peaks merge and were argued to be the reason for the absence of double peak structure at $l = 1 - 2$.

## V. CAE NONLINEAR EVOLUTION

There are few known publications where the nonlinear aspects of CAE evolution were considered as we briefly list in here although this area is largely unexplored. A pioneering study was done in Ref.[57] (main results are summarized in Ref.[8]). The study was focused on the trapped fast ion excitation of some compressional mode characterized by the magnetosonic polarization. The evolution of the CAE mode was considered for the initial stage of the instability in which the EP velocity distribution function is given by the source distribution, which represents a shifted Maxwellian distribution in velocities. Because of this assumption, the considered case can be applicable to the initial stage of the discharge or to when the plasma is heated quickly and alphas do not slow down. The authors concluded, based on numerical results, that the thermal broadening of the $\alpha$-particle source grows logarithmically with time. The considered scenario is not directly applicable to the burning plasmas which are designed for slow evolutions, so that the $\alpha$-particle distribution function remains nearly slowing down at all times[58].

In another publication a set of quasilinear (QL) diffusion equations was considered[59] for the case when the resonance between the oscillations and the fast ions is cyclotron with or without contributions from the EP bounce resonances. The resonance overlap due to Coulomb collisions was also included. The performed theoretical analysis is applicable to the ICRH problem according to that paper and could be used in developing the ICE nonlinear simulations.

Relatively recent studies of ICE in both linear and nonlinear regimes have been done numerically [60, 61]. In those publications particle-in-cell simulations address ICE evolution using the hybrid model computations where ion drift motion is advanced numerically while thermal electrons are treated as a fluid. Simulation allowed the authors to more accurately model both stages of ICE in experiments. In particular, the frequency dependence of expected CAE instabilities had a shape similar to those observed for ICE in JET DT experiments.

## VI. DISCUSSION AND SUMMARY

We over-viewed the linear ICE theory in its present status. ICE theory seems to be sufficiently well developed but needs to be developed further focusing on its potential applications to present day and future experiments on ICE and on its nonlinear aspects. Focusing on experimental studies of ICE will be helpful to unify various existing theories.

It had been theoretically predicted, and now observed experimentally, that many CAE instabilities with narrow spectrum peaks will overlap and form a broader peak near ion cyclotron frequency harmonics. The main difference between more recent observations from STs and those of earlier studies is that the frequency spectrum of observed CAE instabilities in high toroidicity plasma is discrete, so that the properties of each mode can be and were measured separately [17, 62, 63]. In the conventional tokamak ICE was found to consist of the double peaks near each of the cyclotron harmonic as was shown in Ref.[26]. The frequency shift of the instability of those peaks is argued to be due to different signs of the poloidal mode numbers.

From previous studies it is known that due to high magnetic fields in conventional tokamaks the ICE frequency spectrum is populated more densely by the unstable modes. This makes the ST plasma very attractive for studying the properties of individual CAE mode and for verifying the theoretical predictions. In particular, NSTX presents a unique opportunity to study mode numbers, structure, polarization, amplitude etc. We note that, based on CAE observations in NSTX, one would expect that ICE spectrum contains more complicated, fine structures [17, 21] than previously reported [6, 64] perhaps in plasmas with intermediate values of the equilibrium magnetic fields. In addition one should look for the ICE-like high harmonics of the ion cyclotron frequency features in the magnetic activity of STs.

Utilizing ICE theory for EP diagnostics in burning plasma conditions is a challenge facing the EP community. The linear theory as it is outlined above carries the most important elements which is (i) the distribution function of energetic particles. At the moment it is not clear how the distribution function can be extracted from the ICE signal. Dedicated efforts in theory and tokamak experiments are required in order to address the problem. ~~An~~Other items of interest for the community include (ii) the diagnostics of the core plasma and (iii) the phase-space engineering of the EP component of the plasma. ~~Both~~Neither of

these possibilities ~~are not~~ is discussed here.

Nevertheless in connection with ~~the~~ item (i) it seems reasonable to consider linear ICE theory in which ~~can viewed the~~ CAE growth rates can be viewed as a set of EP distribution function moments in velocity space (see Sec.IV). If we assume that the damping rates are small and ICE signal amplitudes are proportional to the growth rates the information about EP distribution function is contained in the growth rate expressions. They are complicated but the very fact that ICE is excited tells us that resonant particles with the source of free energy are present. The shape of ICE spectrum contains more detailed information about the contributions of EP drive and dampings over the velocity space. At this point perhaps the experimental study of ICE especially in STs should be in the focus of the research.

~~The d~~Developing an understanding of ICE for diagnostic purposes in burning plasma conditions makes a perfect case for both the linear and nonlinear development of ICE theory. This was considered in several recent publication, see Refs.[13], and in a recent review [16] in which the summary and current understanding of ICE theory and experiments were included. A pioneering observational analysis from JET by Cottrell pointed out at the proportionality of the ICE signal to the neutron flux over six orders of magnitude of its amplitude[6]. Another example was discussed recently on the ICE activity in DIII-D experiments in which its signals were observed in clear correlation with the off-axis fishbones [65]. Such correlations serve as a compelling case for using ICE for fusion products diagnostics (see Fig.15 f with the Mirnov pick-up coil data in that paper).

A f~~F~~urther idea of interest in connection~~s~~ wtih the ICE problem is ~~the~~ anomalous thermal ion heating, i.e. energy channeling, pointed out in Ref.[66]. In that paper, CAEs were proposed as mediators for energy channeling from the fast ions to thermal ions. In this mechanism, fast ions excite the CAE modes during NBI heating as demonstrated in NSTX. The modes in turn stochastically transfer their wave energy to thermal plasma ions due to the cyclotron damping. Recently, some dedicated studies use the special CAE to KAW decoupling technique [67] to verify the theoretical predictions. Using model parameters, the paper demonstrates the feasibility of this technique and states that more detailed experimental observations of CAE internal amplitudes are required for validations of this idea.

A similar idea of thermal ion anomalous energy diffusion and associated plasma heating is behind the so-called "alpha channeling" [68] when certain plasma oscillations are excited

by the external antennae. Recently, CAEs were suggested to explain strong fast ion energy diffusion in TFTR [69] which was required for alpha channeling to work [56, 70]. This argument pointed to further experiments, even on existing devices, that might verify and further extend this very unusual, but possibly extremely useful, alpha-channeling effect. Moreover, the demonstration of the role played by these modes, together with their theoretical description, carries significant implications for how this effect might be extrapolated with confidence to achieve significant improvements in the tokamak reactor concept. Since this mechanism could mean a big reduction in the cost of electricity produced by fusion, the newly inspired confidence in extrapolating these results may lead to important follow up experiments.

Finally the coupling of CAEs to KAW [37] accounts for anomalous electron thermal transport observed in NSTX [71]. The deficit of heating thermal electrons could account for up to $30-40\%$ of the total NSTX electron transport. In the core of Ref.[37] explanation is the heating power channeling by means of CAE/KAW coupling of thermal electrons. The short wavelength KAW is prone to have a strong parallel electric field and thus very effectively heat thermal electrons. The KAW was found by the HYM code to be localized poloidally on HFS and is in local resonance with CAEs. The radial width of the KAW is comparable to the beam ion Larmor radius. Although the coupling of CAEs and KAWs is demonstrated there is no theoretical explanation of this effect beyond the heuristic consideration offered in our review in Sec. (III).

---


[1] L. V. Korablev and L. I. Rudakov, Zh.Eksp.Teor.Fiz. (Sov. Journal Exp. Theor. Phys.) **54**, 818 (1968).

[2] V. S. Belikov, Y. I. Kolesnichenko, and V. N. Oraevskii, Zh. Eksp. Teor. Fiz. **55**, 2210 (1968).

[3] T. D. Kaladze and A. B. Mikhailovskii, Fizika Plazmy **1**, 238 (1975).

[4] T. D. Kaladze and A. B. Mikhailovskii, Nucl. Fusion **17**, 729 (1977).

[5] W. W. Heidbrink and G. J. Sadler, Nucl. Fusion **34**, 535 (1994).

[6] G. A. Cottrell, V. P. Bhatnagar, O. D. Costa, R. O. Dendy, J. Jacquinot, K. G. McClements, D. C. McCune, M. F. F. Nave, P. Smeulders, and D. F. H. Start, Nucl. Fusion **33**, 1365 (1993).

[7] K. Saito, R. Kumazawa, T. Seki, H. Kasahara, G. Nomura, F. Shimpo, H. Igami, M. Isobe, K. Ogawa, K. Toi, M. Osakabe, M. Nishiura, T. Watanabe, S. Yamamoto, M. Ichimura,

T. Mutoh, and LHD Experiment Group, Plasma Sci. Technol. **15**, 209 (2013).

[8] A. B. Mikhailovskii, *Reviews of Plasma Physics*, **9**, 103 (1986).

[9] S. Cauffman, R. Majeski, K. G. McClements, and R. O. Dendy, Nucl. Fusion **35**, 1597 (1995).

[10] T. Fülöp, , and M. Lisak, Nucl. Fusion **38**, 761 (1998).

[11] Y. I. Kolesnichenko, M. Lisak, and D. Anderson, Nucl. Fusion **40**, 1419 (2000).

[12] R. O. Dendy, C. N. Lashmore-Davies, K. G. McClements, and G. A. Cottrell, Phys. Plasmas **1**, 1918 (1994).

[13] R. O. Dendy and K. G. McClements, Plasma Phys. Control. Fusion **57**, 044002 (2015).

[14] K. G. McClements, R. D´Inca, R. O. Dendy, L. Carbajal, S. C. Chapman, J. W. S. Cook, R. W. Harvey, W. W. Heibrink, and S. D. Pinches, Nucl. Fusion **55**, 043013 (2015).

[15] R. O. Dendy, C. N. Lashmore-Davies, G. A. Cottrell, K. G. McClements, and K. F. Kam, Fusion Technol. **25**, 334 (1994).

[16] N. N. Gorelenkov, S. D. Pinches, and K. Toi, Nucl. Fusion **54**, 125001 (2014).

[17] E. D. Fredrickson, N. N. Gorelenkov, C. Z. Cheng, R. Bell, D. Darrow, D. Johnson, S. Kaye, B. LeBlanc, J. Menard, S. Kubota, and W. Peebles, Phys. Rev. Lett. **87**, 145001 (2001).

[18] N. N. Gorelenkov, C. Z. Cheng, E. D. Fredrickson, E. Belova, D. Gates, S. Kaye, G. J. Kramer, R. Nazikian, and R. B. White, Nucl. Fusion **42**, 977 (2002).

[19] N. N. Gorelenkov, E. Belova, H. L. Berk, C. Z. Cheng, E. D. Fredrickson, W. W. Heidbrink, S. Kaye, and G. J. Kramer, Phys. Plasmas **11**, 2586 (2004).

[20] E. D. Fredrickson, N. N. Gorelenkov, and J. Menard, Phys. Plasmas **11**, 3653 (2004).

[21] L. C. Appel, T. Fülöp, M. J. Hole, H. M. Smith, S. D. Pinches, R. G. L. Vann, and The MAST Team, Plasma Phys. Control. Fusion **50**, 115011 (2008).

[22] H. J. C. Oliver, S. E. Sharapov, R. Akers, I. Klimek, M. Cecconello, and The MAST Team, Plasma Phys. Control. Fusion **56**, 125017 (2014).

[23] S. M. Mahajan and D. W. Ross, Phys. Fluids **26**, 2561 (1983).

[24] B. Coppi, S. Cowley, R. Kulsrud, P. Detragiache, and F. Pegoraro, Phys. Fluids **29**, 4060 (1986).

[25] N. N. Gorelenkov and C. Z. Cheng, Nucl. Fusion **35**, 1743 (1995).

[26] T. Fülöp, Y. I. Kolesnichenko, M. Lisak, and D. Anderson, Nucl. Fusion **37**, 1281 (1997).

[27] Y. I. Kolesnichenko, T. Fülöp, M. Lisak, and D. Anderson, Nucl. Fusion **38**, 1871 (1998).

[28] M. N. Rosenbluth, H. L. Berk, J. W. Van Dam, and D. M. Lindberg, Phys. Rev. Lett. **68**,

596 (1992).

[29] F. Zonca and L. Chen, Phys. Rev. Lett. **68**, 596 (1992).

[30] N. N. Gorelenkov, E. D. Fredrickson, E. Belova, C. Z. Cheng, D. Gates, S. Kaye, and R. B. White, Nucl. Fusion **43**, 228 (2003).

[31] E. D. Fredrickson, N. N. Gorelenkov, M. Podestá, A. Bortolon, N. A. Crocker, S. P. Gerhardt, R. E. B. A. Dialo, B. LeBlanc, F. M. Levinton, and H. Yuh, Phys. Plasmas **20**, 042112 (2013).

[32] N. N. Gorelenkov, C. Z. Cheng, and E. Fredrickson, Phys. Plasmas **9**, 3483 (2002).

[33] H. Smith, T. Fülöp, M. Lisak, and D. Anderson, Phys. Plasmas **10**, 1437 (2003).

[34] N. Gorelenkov, E. Fredrickson, W. Heidbrink, N. Crocker, S. Kubota, and W. Peebles, Nucl. Fusion **46**, S933 (2006).

[35] T. Hellsten and M. Laxåback, Phys. Plasmas **10**, 4371 (2003).

[36] H. M. Smith and E. Verwichte, Plasma Phys. Control Fusion **51**, 075001 (2009).

[37] E. V. Belova, N. N. Gorelenkov, E. D. Fredrickson, K. Tritz, and N. A. Crocker, Phys. Rev. Lett. **115**, 015001 (2015).

[38] N. A. Crocker, E. D. Fredrickson, N. N. Gorelenkov, W. A. Peebles, S. Kubota, R. E. Bell, A. Diallo, B. P. LeBlanc, J. E. Menard, M. Podesta, K. Tritz, and H. Yuh, Nucl. Fusion **53**, 043017 (2013).

[39] S. E. Sharapov, M. K. Lilley, R. Akers, N. Ben Ayed, M. Cecconello, J. W. S. Cook, G. Cunningham, E. Verwichte, and The MAST Team, Phys. Plasmas **21**, 082501 (2014).

[40] T. Fülöp, M. Lisak, Y. I. Kolesnichenko, and D. Anderson, Phys. Plasmas **7**, 1479 (2000).

[41] A. Hasegawa and L. Chen, Phys. Rev. Letter **35**, 370 (1975).

[42] M. N. Rosenbluth and P. H. Rutherford, Phys. Rev. Lett. **34**, 1428 (1975).

[43] J. R. Johnson and C. Z. Cheng, Geophys. Res. Lett. **24**, 1423 (1997).

[44] G. Y. Fu, H. L. Berk, and A. Pletzer, Phys. Plasmas **12**, 082505 (2005).

[45] D. G. Swanson, *Plasma Waves*, 2nd ed. (IOP Publishing, London, 2003).

[46] C. R. Sovinec, "Note on kinetic Alfvén waves," (2009), preprint: UW-CPTC 09-2.

[47] A. Hasegawa and L. Chen, Phys. Fluids **19**, 1924 (1976).

[48] N. N. Gorelenkov and C. Z. Cheng, Phys. Plasmas **2**, 1961 (1995).

[49] N. A. Umov, Zeitschrift für Mathematik und Physik **19**, 97 (1874).

[50] J. H. Poynting, Philosophical Transactions of the Royal Society of London **175**, 343 (1884).

[51] B. Coppi, G. Penn, and C. Riconda, Ann. Phys. **261**, 117 (1997).

[52] G. Penn, C. Riconda, and F. Rubini, Phys. Plasmas **5**, 2513 (1998).

[53] V. S. Belikov, Y. I. Kolesnichenko, and O. A. Silivra, Nuclear Fusion **35**, 1603 (1995).

[54] V. S. Belikov, Y. I. Kolesnichenko, and R. B. White, Phys. Plasmas **10**, 4771 (2003).

[55] V. S. Belikov, Y. I. Kolesnichenko, and R. B. White, Phys. Plasmas **11**, 5409 (2004).

[56] N. N. Gorelenkov, N. J. Fisch, and E. Fredrickson, Plasma Phys. Control. Fusion **52**, 055014 (2010).

[57] A. B. Mikhailovskii, D. G. Lominadze, and T. D. Kaladze, Preprint, IAE- **2981** (1978).

[58] R. V. Budny, Nucl. Fusion **49**, 085008 (2009).

[59] V. S. Belikov and Y. I. Kolesnichenko, Plasma Phys. Control. Fusion **36**, 1703 (1994).

[60] J. W. S. Cook, R. O. Dendy, and S. C. Chapman, Plasma Phys. Control. Fusion **55**, 065003 (2013).

[61] L. Carbajal, R. O. Dendy, S. C. Chapman, and J. W. S. Cook, Phys. Plasmas **21**, 012106 (2014).

[62] E. D. Fredrickson, R. E. Bell, D. Darrow, G. Fu, N. N. Gorelenkov, B. P. LeBlanc, S. S. Medley, J. E. Menard, H. Park, A. L. Roquemore, W. W. Heidbrink, S. A. Sabbagh, D. Stutman, K. Tritz, N. A. Croacker, S. Kubota, W. Peebles, K. C. Lee, and F. M. Levinton, Phys. Plasmas **13**, 056109 (2006).

[63] N. A. Crocker, E. D. Fredrickson, N. N. Gorelenkov, W. A. Peebles, S. Kubota, R. E. Bell, B. P. LeBlanc, J. E. Menard, M. Podesta, K. Tritz, and H. Yuh, in *Proceedings of 24th IAEA Fusion Energy Conference, San Diego, USA*, IAEA-CN-197/EX/P6-02 (2012).

[64] S. Cauffman and R. Majeski, Rev. Sci. Instrum. **66**, 817 (1995).

[65] W. W. Heidbrink, M. E. Austin, R. K. Fisher, M. García Muñoz, G. Matsunaga, G. R. McKee, R. A. Moyer, C. M. Muscatello, M. Okabayashi, D. C. Pace, K. Shinohara, W. M. Solomon, E. J. Strait, M. A. Van Zeeland, and Y. Zhu, Plasma Phys. Control. Fusion **53**, 085028 (2011).

[66] D. Gates, N. N. Gorelenkov, and R. B. White, Phys. Rev. Lett. **87**, 205003 (2001).

[67] H. M. Smith, D. A. Gates, N. N. Gorelenkov, R. B. White, and E. Fredrickson, in *41st European Physical Society Conference on Plasma Physics*, P2.019 (European Physical Society, 2014).

[68] N. J. Fisch and J.-M. Rax, Phys. Rev. Lett. **69**, 612 (1992).

[69] D. Darrow, R. Majeski, N. J. Fisch, R. Heeter, H. Herrmann, M. Herrmann, M. Zarnstorff, and S. Zweben, Nucl. Fusion **36**, 509 (1996).

[70] D. S. Clark and N. J. Fisch, Phys. Plasmas **7**, 2923 (2000).

[71] D. Stutman, L. Delgado-Aparicio, N. Gorelenkov, M. Finkenthal, E. Fredrickson, S. Kaye, E. Mazzucato, and K. Tritz, Phys. Rev. Lett. **102**, 115002 (2009).

PPPL PRINCETON PLASMA PHYSICS LABORATORY

# Princeton Plasma Physics Laboratory
# Office of Reports and Publications

Managed by
Princeton University

under contract with the
U.S. Department of Energy
(DE-AC02-09CH11466)

P.O. Box 451, Princeton, NJ 08543
Phone: 609-243-2245
Fax: 609-243-2751

E-mail: publications@pppl.gov

Website: http://www.pppl.gov